[Cancer Biology & Therapy 4:2, 197-206, February 2005]; ©2005 Landes Bioscience

Research Papers

Mitotic Spindle Checkpoint Inactivation by Trichostatin A Defines a Mechanism for Increasing Cancer Cell Killing by Microtubule-Disrupting Agents

Melissa Dowling
K. Ranh Voong
Mijin Kim
Michael K. Keutmann
Eleanor Harris
Gary D. Kao*

Departments of Radiation Oncology; Philadelphia Veterans Affairs Medical Center and the University of Pennsylvania School of Medicine; Philadelphia, Pennsylvania USA

*Correspondence to: Gary D. Kao; University of Pennsylvania School of Medicine; John Morgan 180 H; Philadelphia, Pennsylvania 19104 USA; Tel.: 215.573.5503; Fax: 215.898.0090; Email: Kao@xrt.upenn.edu

Received 10/26/04; Accepted 12/08/04

Previously published online as a *Cancer Biology & Therapy* E-publication: http://www.landesbioscience.com/journals/cbt/abstract.php?id=1441

KEY WORDS

spindle-checkpoint, paclitaxel, microtubule disruption, trichostatin A, TSA, cell cycle.

ACKNOWLEDGEMENTS

We are grateful to the other members of the Kao laboratory for technical assistance and comments, including Dr. Mijin Kim, Anil Magge, Katie Murphy, Wes Baff, and Shary Parker. We thank Dr. Tim J. Yen for helpful comments during the beginning stages of this work. We especially thank Dr. Gordon Chan and Dr. Yen for generously sharing reagents.

This work was supported by funds from the W.W. Smith Charitable Trust, the Office of Research and Development Medical Research Service, Department of Veterans Affairs (Advanced Career Research Award) (to G.D.K.), and the National Institutes of Health (CA107956-01) (to G.D.K.).

SUPPLEMENTARY MATERIAL

Supplemental Fig. 1S can be found at: http://www.landesbioscience.com/journals/cbt/dowling4-2-sup.pdf.

ABSTRACT

Microtubule-disrupting agents such as the taxanes comprise some of the most clinically useful chemotherapeutic agents and invoke the spindle checkpoint in proliferating cells. A robust spindle checkpoint in turn may forestall mitotic catastrophe, potentially providing a mechanism that permits cancer cells to survive transient exposure to these drugs. Previous reports on G_2-M cell cycle progression by histone deacetylase inhibitors suggested a potential role in modulating the therapeutic efficacy of microtubule-disrupting agents. As both classes of agents are generally administered in clinical trials as pulse treatments, we investigated in human cancer cells the effects of brief treatments with the histone deacetylase inhibitor trichostatin A (TSA) alone or with nocodazole or paclitaxel (Taxol) on cell cycle progression and the spindle checkpoint. Treatment of synchronized cells with 200 ng/ml of TSA alone for eight hours to completely block class I and II HDACs did not interfere with progression into mitosis with chromosomal condensation as confirmed by MPM-2 expression. TSA treatment at this concentration surprisingly did not interfere with formation of the mitotic spindle or centrosomal separation, but instead led to missegregation of chromosomes, suggesting effects on the spindle checkpoint. Consistent with this hypothesis, TSA abrogated the phosphorylation and kinetochore localization of the mitotic checkpoint protein BubR1 and the phosphorylation of histone H3 after paclitaxel and nocodazole treatment. These effects in turn led to rapid cell death and considerably reduced clonogenic survival. These results together suggest that by inactivating the spindle checkpoint, TSA can potentiate the lethal effects of microtubule-disrupting drugs, a strategy that might be usefully exploited for optimizing anticancer therapy.

INTRODUCTION

Mitosis is a highly complex and regulated process, with failsafe mechanisms that ensure proper alignment of the chromosomes at the metaphase plate and equal congression of the chromosomes to daughter cells, (reviewed in refs. 1–3). These checkpoint mechanisms control the progression of mitosis by invoking a cell cycle delay when conditions are not quite "right", therefore preventing the potentially catastrophic consequences that might result when cells with unaligned chromosomes prematurely enter anaphase. While a mitotic checkpoint may be enforced at a number of discrete times during the cell cycle progression from prophase through anaphase, probably the best characterized checkpoint is that mediated through mechanisms that sense the attachment of microtubules of the mitotic spindle to the kinetochore or the tension that results after such attachment. The mitotic "spindle checkpoint" therefore serves to time chromosomal congression only after the chromosomes have completely and equally aligned at the metaphase plate. The sensitivity of the spindle checkpoint is such that a single unaligned chromosome is sufficient to prevent completion of mitosis.[4] A robust mitotic spindle checkpoint potentially allows time to repair chromosomal damage and effect their proper alignment, while in contrast, inactivation or targeted disruption of the spindle checkpoint leads to rapid cellular death.[5,6]

The molecular mechanisms of the spindle checkpoint have implicated the activity of mitotic checkpoint proteins encoded by the *BUB* and *MAD* genes, including as BubR1, Bub1, Bub3, Mad1, and Mad2.[4,7-13] A number of drugs of clinical and biomedical research importance disrupt the assembly (e.g., nocodazole and vincristine) or disassembly (e.g., paclitaxel and docetaxel) of microtubules and in doing so, invoke the spindle checkpoint. When microtubule dynamics are disrupted by these drugs, the mitotic checkpoint proteins localize prominently to the kinetochores, where a wait signal that inhibits the

Anaphase Promoting Complex/Cyclosome (APC/C) is transmitted and which in turn forestalls the degradation of proteins such as cyclin B1 which must be degraded in order for anaphase to proceed.[14] Because paclitaxel and docetaxel are among the most important chemotherapeutic agents used to treat patients with cancer, strategies or agents that enhance their efficacy would be greatly welcomed.

By inhibiting the deacetylation of core histones, histone deacetylase inhibitors potentially influence the structure of chromatin.[15-17] Trichostatin A (TSA) is a histone deacetylase inhibitor (HDI) that affects both class I and II HDACs, with a higher concentration (> 100 nM of TSA) required to completely inhibit Class II HDACs such as HDAC4.[18] The HDI's have been previously noted to affect both G_1 and G_2/M cell cycle progression. While the G_1 block has been attributed to repression of transcription or induction by HDI of the cyclin-dependent kinase inhibitor p21,[19-23] comparatively less is known about the mechanisms involved in the perturbation of G_2/M progression by HDIs. Cimini et al.[24] found evidence of impaired chromatin condensation and delayed mitotic progression in cells treated with TSA, and which was associated with lagging chromosomes and chromatin bridges in about 1–2% of treated human fibroblasts.[24] Warrener, et al.[25] found increased cell death in cells treated with an HDI unrelated to TSA, azelaic bishydroxamic acid (ABHA).[25] While the HDIs have shown activity in clinical trials in which these agents have been given as pulse treatments, it has been proposed that the anticancer efficacy of these drugs may be especially enhanced when combined with other cytotoxic agents.[26-33] We therefore investigated the effects on cell cycle progression into mitosis and clonogenic survival of brief exposure to a concentration of TSA sufficient to fully block histone deacetylation. To better characterize relatively unexplored aspects of TSA effects on mitotic progression, we assessed mitotic spindle and centrosome formation and localization, as well as the phosphorylation and localization of the BubR1 mitotic checkpoint protein, key determinants of intact spindle checkpoint function.[34-36] Finally, to further broaden the therapeutic relevance of our findings, the effect of brief TSA treatment on mitotic checkpoint function in the presence of microtubule-disrupting drugs was then investigated.

MATERIALS AND METHODS

All cell lines cells were obtained from the American Type Culture Collection (ATCC) (Manassas, VA, USA), and grown in DMEM media (Gibco/BRL) supplemented with 15% fetal bovine serum (FBS) at 37°C in 5% CO_2. Nocodazole, aphidicolin and trichostatin A (TSA) were obtained from Sigma (St. Louis, MO, USA), and prepared as 1000X stock in DMSO. For experiments, these were diluted in media, and used at concentrations and conditions as previously described or noted in the figure legends.[37] Nocodazole was used at 0.1 μM, paclitaxel was used at 20 nM, while trichostatin A (TSA) was used at 200 ng/ml to completely block both Class I and II HDAC activity.[18] Mock-treated control cells were handled in an identical manner to experimental samples, with an identical amount of media added (without drug). In experiments in which cells were synchronized, this was accomplished via aphidicolin synchrony as previously described.[39] Colony survival assays were performed by treating synchronized cells with TSA three hours after release, either alone or followed by the addition of nocodazole or paclitaxel. The drugs were subsequently removed from the cells by washing with phosphate buffered saline (PBS) for three times, followed by counting via serial dilutions and then plating in triplicate into fresh plates with media free of drugs and left to grow undisturbed for ten days in the incubator. Colonies were subsequently fixed and stained with crystal violet in methanol, and scored as those containing 75 or more cells. Colonies counts were normalized to control (mock-treated), and expressed as a percentage.

For immunoblotting cell lysates were prepared via harvesting and pelleting cells in extraction buffer containing 10 mM HEPES, pH 7.9, 1.5 mM $MgCl_2$, 10 mM KCl, .5 mM DTT and 1.5 mM PMSF, followed by resuspension in Laemmli buffer and ultrasonic sonication for 10 cycles. Samples were boiled for 5 minutes prior to loading (10 μg/lane) and separating via SDS-polyacrylamide gel electrophoresis (SDS-PAGE), and transferring to nitrocellulose membranes. Studies to confirm protein phosphorylation was performed by treating the cell lysates with protein phosphatase at (5 U) for 10 minutes at 37° before boiling. After transfer, the membranes were blocked with 5% nonfat milk in phosphate-buffered saline (PBS), and then probed with the indicated primary antibodies, followed by the appropriate secondary antibodies conjugated with horseradish peroxidase. Washes were performed with PBS with 0.1% Tween. Finally, membranes were exposed to film after enhanced chemilluminescence (ECL) (Amersham Biosciences, Piscataway, NJ, USA). Anti-histone H3 and H4 (total and acetylated), anti-phosphorylated histone H3 (both at Serine 10 and Serine 28) and MPM2 antibodies were from Upstate Biotechnology. Anti-cyclin B1 antibody was from BD Pharmingen. Anticentromere autoimmune serum was a gift of K. Sullivan (Scripps Research Institute, La Jolla, CA), and were used at 1:2000. Anti-BubR1 antibodies, a kind gift from Drs. Gordon Chan and Tim Yen were used at 1:1000.

Immunofluorescence and fluorescence-activated cell sorting (FACS) analysis of DNA content was performed as previously described.[39] During the FACS, no gating was performed on the propidium iodide (PI)-stained nuclei, in order that all cells were included in the analysis, especially those with sub-G_1 content representative of nuclear fragmentation. Prior to staining of the nuclei, cells with sub-G_1 content were confirmed to be nonviable through Trypan blue and propidium iodiden (PI) exclusion assays. For immunofluorescence, cells grown on coverslips were fixed in ice-cold acetone: methanol (50:50), washed in phosphate-buffered saline and KB buffer (50 mM TRIS-HCl pH 7.4, 150 mM NaCl, 0.1% BSA), prior to labeling with specific antibodies. The respective primary antibody that was then detected via the species-specific secondary antibody conjugated to Alexa Fluor 594 or 488 (Molecular Probes, Eugene, OR). DNA was stained with 0.1 mg/ml of 4', 6-diamidino-2-phenylindole (DAPI, Sigma). The coverslips were then mounted in 0.1% para-phenylenediamine in glycerol. Stained cells were examined with a 100X PlanNeofluor objective mounted on a Nikon TE-200 microscope equipped with epifluorescence optics. Images were captured with a Hammamatsu CCD camera that was controlled with IP LabSpectrum v2.0.1 (Scanalytics Inc.).

RESULTS

Cell cycle progression after timed TSA treatment. We first established the response of unsynchronized Hela cells to TSA. TSA treatment for 12 hours results in accumulation of cells with G_1 and G_2/M DNA content (Fig. 1A and B), consistent with previously published reports.[20,21,25] To focus on the effect of TSA treatment on the G_2 to mitosis progression, we synchronized Hela cells via aphidicolin-induced G_1/S cell cycle block, which enables the analysis of 75% or more of the cells traversing the cell cycle in unison.[39,40] The synchronized cells were then released, and mock-treated or treated with TSA three hours after release, when they had largely progressed into S phase (experimental schema as shown in Figure 2A. Cells were harvested at successive time-points thereafter, and assessed for DNA content (Fig. 2B) or protein expression (Fig. 2C). TSA did not appreciably perturb progression through interphase into G_2/M under these conditions, nor inhibited chromosomal condensation in mitosis (Supplemental Fig. 1S). To confirm that the TSA-treated cells had indeed progressed into mitosis, we probed cell lysates for cyclin B1 protein and the MPM2 mitotic epitope, in addition to confirming histone hyperacetylation due to the inhibition of histone deacetylase activity by TSA. Cyclin B1 is maximally expressed by G_2/M cells and this as well as MPM2 reactivity was evident in both mock-treated control cells as well as cells treated with TSA, supporting that cell cycle progression into G_2 and mitosis was not inhibited by TSA.

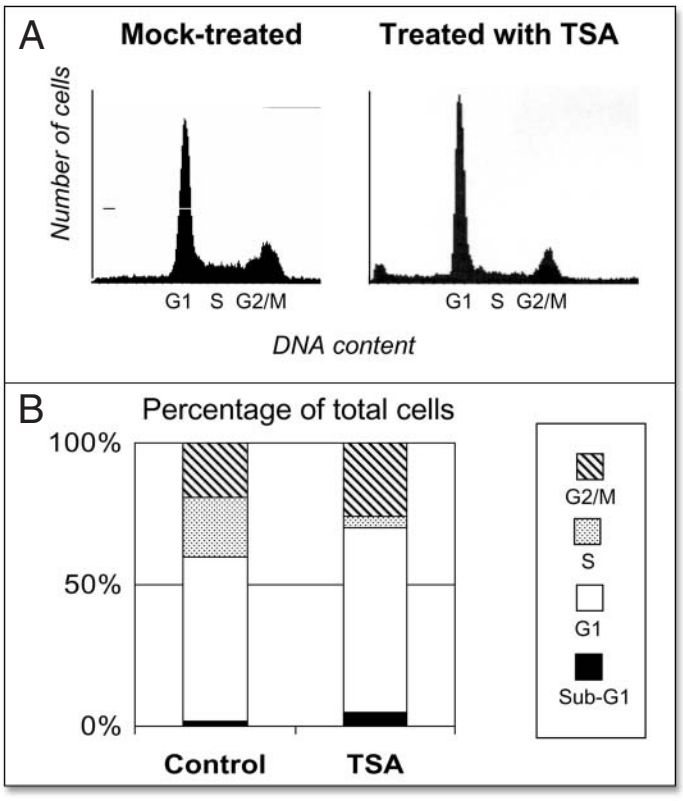

Figure 1. Brief treatment of Hela cells with TSA results in accumulation of cells with G_1 and G_2/M DNA content. (A) Asynchronous Hela cells were mock-treated or treated with TSA for eight hours, and analyzed for DNA content via FACS. The resulting histograms are shown, with the G_1, S and G_2/M regions indicated. (B) Bar graphs showing the cell-cycle distribution of cells in each treatment group in the histograms shown in (A).

The major effect of TSA emerged later, when the control mock-treated cells had largely completed mitosis and returned to G_1 (20 hours after release). In contrast to the control cells, significantly fewer cells treated with TSA had returned to G_1, with a proportion of treated cells reaching prophase uneventfully, but then subsequently undergoing nuclear fragmentation while in mitosis, finally resulting in cells with sub-G_1 DNA content (Fig. 2D and E).

Mitotic spindle formation and centrosomal localization after TSA treatment. These results suggested that TSA might be affecting specific cellular events that are characteristic of mitosis. We began by assessing the formation of the mitotic spindle, perhaps the most dramatic mitotic structure, in control and treated cells. Mock-treated control cells as expected showed spindle formation (Fig. 3A, left column), with the mitotic spindles bisected by the aligned chromosomes in metaphase or by congressed chromosomes in anaphase. Spindle formation surprisingly was also detectable in the TSA-treated cells, including clearly bipolar spindles reminiscent of the mock-treated controls. However, in contrast to the controls, the chromosomes of the TSA treated cells were often unaligned at the metaphase plate or unevenly segregated (Fig. 3A, right column). These abnormalities persisted as many cells at later times did not show reversion to a pattern consistent with orderly segregation, but instead showed progressively increased degrees of nuclear fragmentation and death (Supplemental Fig. 1SC and results not shown).

We investigated next whether the missegregation seen after TSA treatment might be related to defects in centrosomal formation. However, in both mock-treated control cells as well as TSA-treated cells, the centrosomes localized to the polar ends of the mitotic spindle, and TSA-treated cells showed robust staining of gamma-tubulin (Fig. 3B). These results together suggested that mitotic catastrophe seen after TSA treatment was not due to impaired mitotic spindle formation or centrosomal localization.

Inhibition of BubR1 and histone H3 phosphorylation by TSA. The missegregation of chromosomes in the context of intact spindles seen with TSA suggested a possible defect in the spindle checkpoint that would otherwise prevent missegregation due to inappropriate chromosome congression. We began by assessing for structural determinants of the spindle checkpoint, including the phosphorylation of histone H3 in mitosis and the kinetochore localization of the checkpoint protein BubR1. During mitosis, when transcription is globally repressed, histone H3 is deacetylated but phosphorylated.[16,40-44] Phosphorylation of histone H3 at serine 28 has been described as a mitotic specific-event in human cells.[45,46] Phosphorylation of histone H3 appears to be coincident with and possibly facilitates the phosphorylation and recruitment to kinetochores of the mitotic checkpoint protein BubR1.[8-12] Consistent with a link between phosphorylation of histone H3 and activation of BubR1, inhibition of the kinase, that phosphorylates histone H3, Aurora B kinase not only results in diminished histone H3 phosphorylation, but also impairs the localization and activity of BubR1 at the kinetochore during mitosis.[34-36]

We found brief TSA treatment of synchronized cells did not impair chromosomal condensation during the entry into mitosis, but inhibited the phosphorylation of histone H3 in these cells (Fig. 4A, right panels, compare with mock-treated control cells in left panels). Next, we stained for BubR1 protein after mock and TSA treatment. BubR1 localization to paired kinetochores was readily apparent in mitotic control cells. In contrast, in TSA treated mitotic cells, much less BubR1 staining at kinetochores could be detected and very few showed the conspicuous localization of BubR1 to paired kinetochores that was seen in control cells (Fig. 4B, left versus right panels).

We repeated the experiment to obtain total cell lysates for immunoblotting. Parallel plates of cells in interphase (6 hours after release from G_1/S block) or in mitosis (12 hours after release) were harvested, and the lysates immunoblotted for phosphorylated histone H3. In control cells phosphorylated histone H3 was detected as expected in mitotic cells but not those in interphase (black filled arrowhead, Fig. 4C) (the results shown are for histone H3 phosphorylated at serine-28, probing for histone H3 phosphorylated at serine-10 showed similar results (not shown). Treatment with TSA resulted in hyperacetylation of histone H3 and H4, again an expected result (open arrowheads, Fig. 4C). However, TSA led to markedly diminished phosphorylated histone H3 in treated mitotic cells (filled arrowhead), in contrast to the strong signal of phosphorylated histone H3 in control mitotic cells. These results together were therefore consistent with the immunofluorescence results, which showed diminished phosphorylated histone H3 in mitotic cells that had been treated with TSA.

We also probed the cell lysates for BubR1. Control mock-treated cells unexposed to TSA showed the slower migrating form of BubR1, consistent with its phosphorylated activated form in mitosis (top bands, Fig. 4B). In contrast, TSA-treated mitotic cells showed only the faster migrating form, suggesting a lack of phosphorylation. To confirm the phosphorylation status of BubR1 in the control cells, we harvested control and TSA-treated cells after passage into mitosis, and treated the respective lysates with protein phosphatase prior to separation via SDS-PAGE. Control cells show the slower migrating form of BubR1 which after phosphatase treatment is largely converted to the faster running unphosphorylated form (Fig. 4D). The cell lysate of the TSA treated cells, in contrast, show no change with phosphatase treatment.

TSA abrogates the spindle checkpoint induced by microtubule-disrupting agents. The inhibition of BubR1 phosphorylation by TSA suggested that its activity might be perturbed, especially during the critical progression into mitosis when the protein contributes to mechanisms that monitor the recruitment of chromosomes to the mitotic spindle. The activity of BubR1 is reflected in its localization to the kinetochore when chromosomes have yet to be properly aligned at the metaphase plate. We therefore assessed the localization of BubR1 in synchronized cells treated briefly with TSA and which were then allowed to progress into mitosis after disruption of microtubules

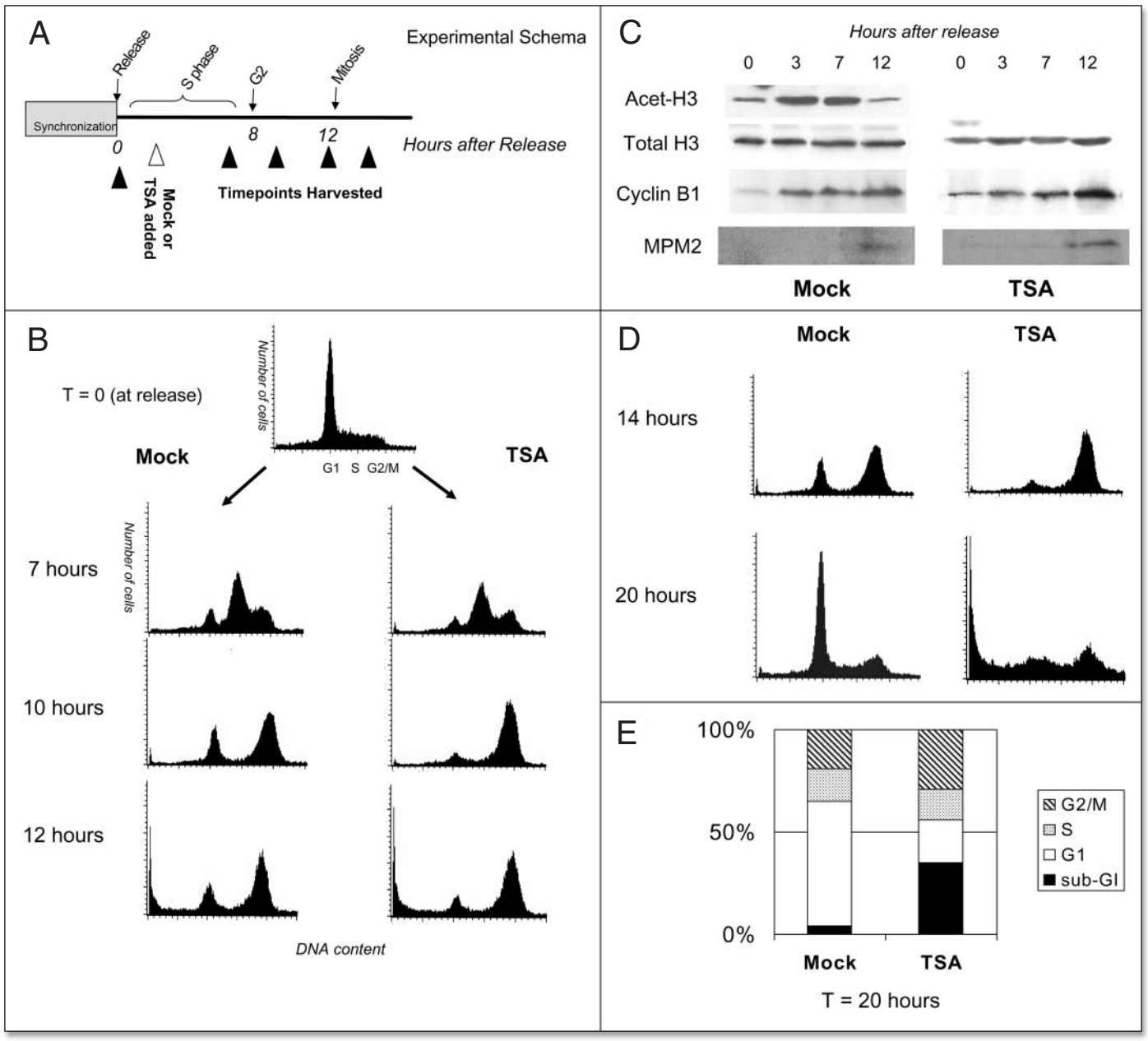

Figure 2. Brief treatment with TSA does not interfere with S phase cell cycle progression, but cell death occurs later. (A) Schema of the experiment. Hela cells were synchronized in G_1/S with aphidicolin. Three hours after release, TSA (200 ng/ml final concentration) was added or the cells were mock-treated (open triangle). Parallel plates of cells in each treatment group were then harvested for analysis of DNA content via FACS (as shown in B) or protein expression via immunoblotting (C) at successive timepoints (indicated by filled triangles) through the remainder of the cell cycle. (B) Histograms showing the cell cycle distribution of cells that were mock-treated or treated with TSA, at release (top histogram), or 7, 10 and 12 hours after release (timepoints indicated in A). The cell cycle distributions between the two treatment groups are almost equivalent during the cell cycle progression from S into G_2/M (corresponding respectively to 7 and 10 hours after release). (C) Immunoblotting of treated cells through the cell cycle. Cells were synchronized and released, and mock-treated or TSA-treated as in (A and B), and harvested at the timepoints indicated. Cell lysates were separated via SDS-PAGE, transferred to nitrocellulose, and probed for the indicated proteins. MPM2 is a standard mitotic marker, and indicates that both mock-treated and TSA-treated cells progress into mitosis. (D) Histograms showing the cell cycle distribution at late time points of cells that were mock-treated or treated with TSA. Cells prepared and treated as in (A) in (B) but harvested at 14 and 20 hours for FACS analysis. A difference between the two treatment groups is most notable at 20 hours after release, at a time when the mock-treated controls have completed and progressed out of mitosis and into G_1. TSA-treated cells enter mitosis, as indicated by the FACS histogram at 12 and 14 hours and the immunoblotting shown in (C). However, in contrast to mock-treated controls, few TSA-treated cells at 20 hours had completed mitosis and returned to G; instead substantial cell death is evident, as indicated by increased proportion of cells with sub-G_1 DNA content, together suggesting cell death occurred during mitosis. (E) Bar graphs showing the cell-cycle distribution of cells in each treatment group at 20 hours after release (histograms shown in D).

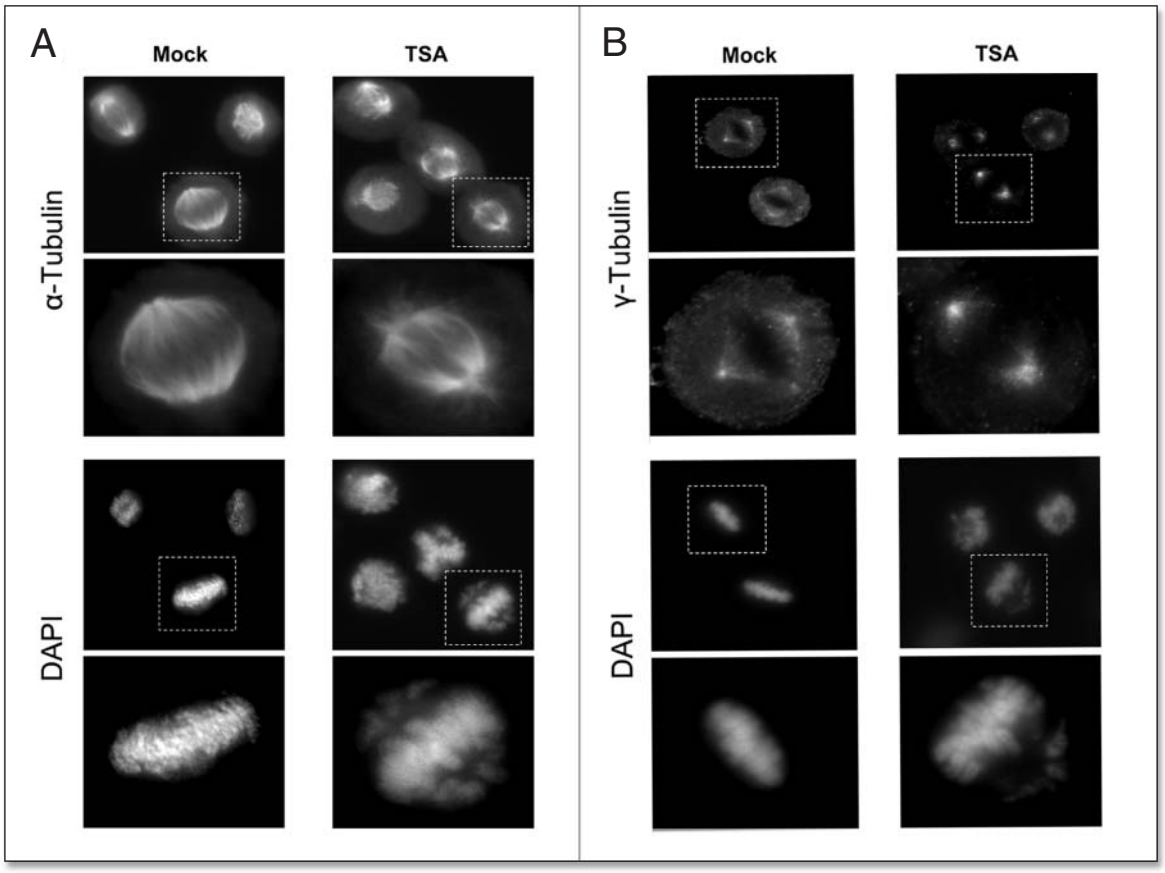

Figure 3. Mitotic spindle formation and centrosomal positioning after brief TSA treatment. (A) Synchronized Hela cells grown on coverslips were mock-treated (left panels) or treated with TSA (right panels) as in Figure 2, fixed twelve hours after release, and stained for α-tubulin (top panels) to assess for the mitotic spindle and DAPI (bottom panels) to visualize the chromosomes condensed in mitosis. Identical groups of cells are shown for each treatment group (e.g., the mock-treated cells stained for α-tubulin in the top panel are identical to the ones stained for DAPI in the third panel). The cells within the dashed box are shown under higher power in the panel immediately below. While both mock- and TSA-treated cells show mitotic spindle formation, the chromosomes in the TSA-treated cells are however frequently misaligned or have missegregated. (B) Cells prepared and treated as in (A). were stained for γ–tubulin to assess for centromes and DAPI to visualize the chromosomes. Identical groups of cells are shown for each treatment group and the cells within the dashed box are shown under higher power in the panel immediately below. Despite the missegregation of chromosomes frequently seen after TSA treatment, bipolar centrosomes are readily detectable.

by nocodazole (Fig. 5A) or paclitaxel (Fig. 5B). Control cells that had progressed into mitosis in the presence of either nocodazole or paclitaxel, as expected, showed robust localization of BubR1 to paired kinetochores in mitotic cells treated with (panels in left column). In contrast, TSA treated cells which had progressed into mitosis showed poor BubR1 localization to kinetochores (panels in right column).

The lack of phosphorylation of BubR1 and its impaired kinetochore localization after brief TSA treatment suggested that the mitotic spindle checkpoint induced by nocodazole or paclitaxel might be impaired. We therefore performed FACS analysis on cells prepared in an identical manner to evaluate the cell cycle response. At 20 hours after release from G_1/S block, control cells challenged with either Nocodazole or Taxol remained blocked in mitosis as expected (Fig. 5C, left upper panels). In contrast, the mitotic checkpoint was considerably abrogated in cells to which TSA had been added after Nocodazole or Taxol (Fig. 5C, right upper panels and Fig. 5D, top graph). TSA led to a decrease in the proportion of cells that remain blocked in mitosis, concomitant with an increase in the proportion of cells with sub-G_1 DNA content. To investigate further the effects of TSA on the spindle checkpoint, we investigated HT29 cells, a colorectal cancer cell line with a very robust mitotic checkpoint. When challenged with either Nocodazole or Taxol, HT29 cells blocked robustly in mitosis, as expected (Fig. 5C, left bottom panels). However, when these cells were treated with TSA after to the addition of Nocodazole and Taxol, a substantial portion of cells were no longer able to remain blocked in mitosis. The reduction in cells blocked in mitosis was again accompanied by an increase in cells with sub-G_1 content (Fig. 5C right bottom panels and Fig. 5D), bottom graph). Together, these results suggest that TSA abrogates the spindle checkpoint, resulting in increased nuclear fragmentation.

Mitotic checkpoint abrogation results in decreased clonogenic survival. The abrogation of the spindle checkpoint by brief TSA exposure led to nuclear fragmentation in a proportion of cells. While it seemed highly unlikely that any surviving cells would subsequently have a growth advantage, we wished to formally test the long-term consequences of TSA treatment via the colony survival assay. This assay is standard measure of clonogenic survival, but also assesses the response of the entire population of treated cells. Brief exposure to TSA resulted in slightly fewer colonies compared to mock treated controls (Fig. 6A and C). Colony formation after brief treatment with TSA or nocodazole alone was also fairly comparable (Fig. 6B and C). In contrast, a considerably larger effect on clonogenic survival was noted when cells were treated with TSA combined with nocodazole or Taxol. With combined treatment each case resulted in substantially fewer colonies than either single treatment (Fig. 6B and C). Together, these results are consistent with the notion that by abrogating the mitotic spindle checkpoint invoked by nocodazole or Taxol, TSA induces rapid nuclear fragmentation and cell death, and reducing the proportion of cells surviving to form colonies.

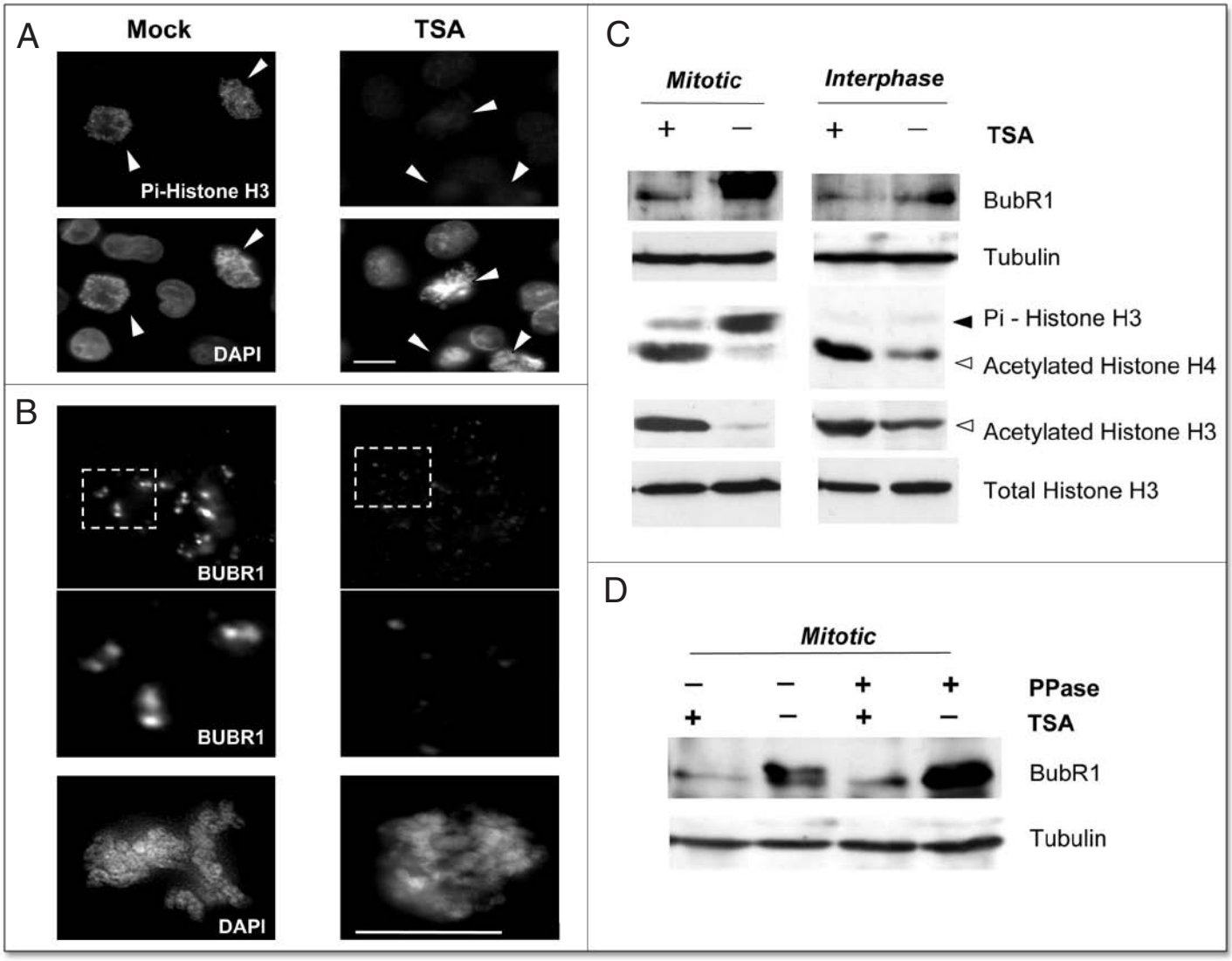

Figure 4. TSA treatment of synchronized cells impairs phosphorylation of histone H3 and BubR1 activity. (A) Hela cells prepared and treated as in Figure 3, were fixed at ten hours after release (when cells have begun to enter mitosis) and stained for Ser-28 phosphorylated histone H3 ("Pi-Histone H3", topmost panels) or DAPI (second row of panels). Pi-histone H3 and DAPI staining in the top two panels are of identical cells. Arrowheads indicated mitotic cells, in which chromatin has condensed. Inactivation of histone deacetylase with TSA does not impede chromatin condensation (as in Fig. 3), but inhibits phosphorylation of histone H3. Images shown of control and TSA-treated cells were captured with equal length of exposure time and are representative of at least 100 cells in each treatment group. Bar, 5 microns. (B) Cells prepared and treated as in (A), but stained for BubR1 (top and middle panels, "BUBR1") and chromatin (bottom panel, "DAPI"). The dashed areas in top panels are enlarged in the middle panels. Control cells show BubR1 localization at the paired kinetochores in mitotic cells, while TSA-treated cells show diminished BubR1 localization. The kinetochore localization of BubR1 coincides with staining using human anti-centromeric sera (results not shown). Images shown of control and TSA-treated cells were captured with equal length of exposure time and are representative of at least 100 cells in each treatment group. Bar, 5 microns. (C) Hela cells were synchronized and treated with TSA (200 ng/ml) three hours after release. Five or twelve hours after release, when the cells were in respectively interphase ("Interphase") or mitosis ("Mitotic"), the cells were harvested and cell extracts separated via SDS-PAGE, transferred to nitrocellulose, and probed for the proteins indicated. TSA in both interphase and mitotic cells led to hyperacetylation of both histones H3 and H4. Mock-treated control cells showed robust expression of phospho-histone H3, but which was diminished in TSA-treated cells. The slower migrating hyperphosphorylated form of BubR1 is seen in control but not in TSA-treated mitotic cells. Probing for α-tubulin and total histone H3 served as loading controls for the immunoblots. In all plates, nocodazole was added seven hours after release from aphidicolin to in order to prevent cells from traversing back to G_1. (D) Phosphorylation of BubR1 during mitosis, and inhibition by TSA treatment. Hela cells were prepared and treated as in (A), but harvested fifteen hours after release in the presence of nocodazole to trap cells in mitosis. Cell lysates were then mock- or treated with protein phosphatase separation via SDS-PAGE, transfer to nitrocellulose, and probing for BubR1 or α-tubulin (as a loading control). Phosphatase results in downshift to the slower migrating forms of BubR1, consistent with hyperphosphorylation during mitosis.

DISCUSSION

The observations we report here extend evidence of the potential therapeutic usefulness of the histone deacetylase inhibitors in a number of novel ways. Through analysis of near-completely synchronized cancer cells, we establish that exposure to TSA does not prevent the cells from traversing interphase and entering mitosis, and subsequently forming mitotic spindles and bipolar centrosomes. However, TSA impairs the phosphorylation and kinetochore localization of the mitotic checkpoint protein BubR1 and which likely

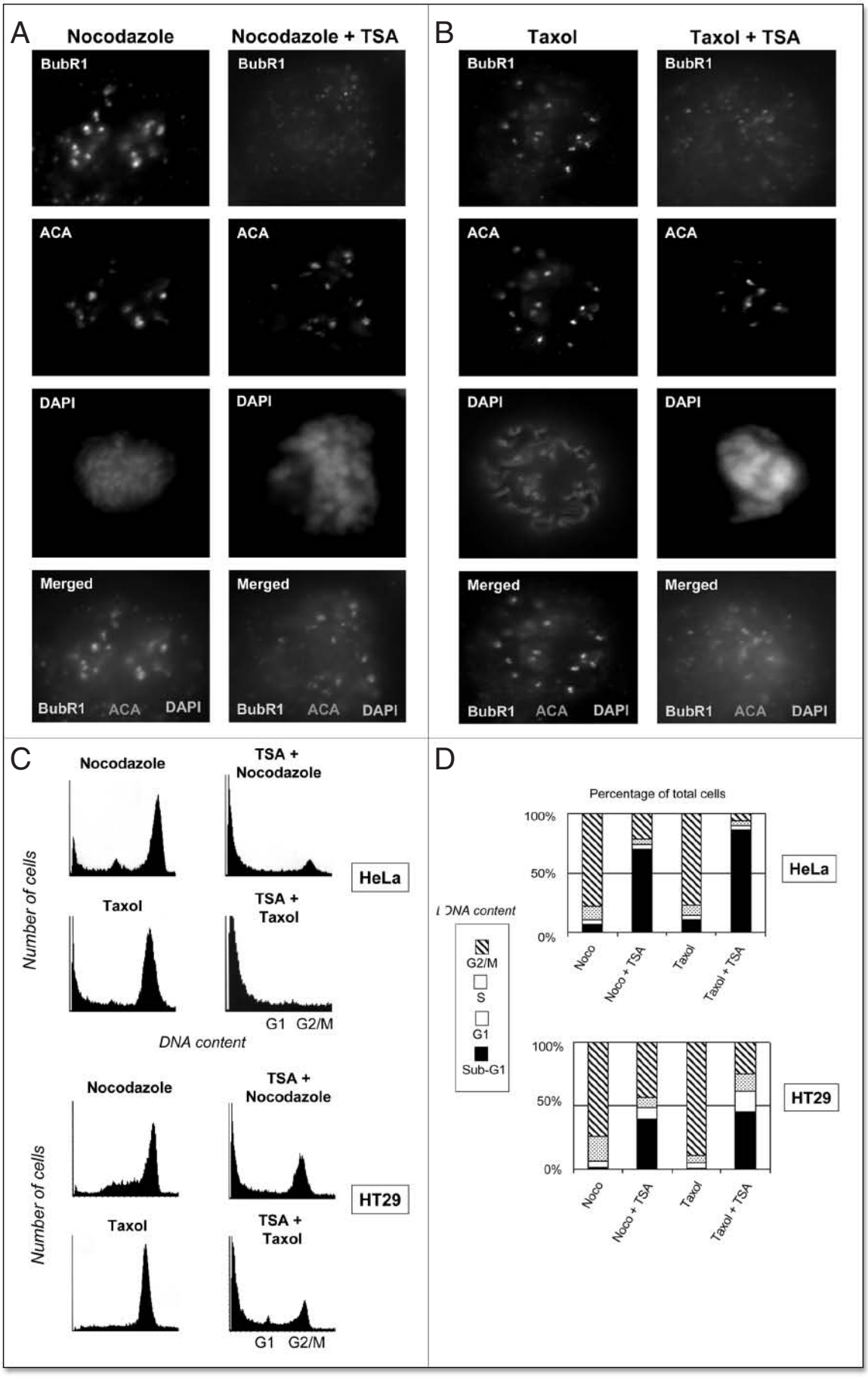
A
Nocodazole
Nocodazole + TSA
BubR1
ACA
DAPI
Merged
BubR1 ACA DAPI
B
Taxol
Taxol + TSA
C
Nocodazole
TSA + Nocodazole
Taxol
TSA + Taxol
Number of cells
HeLa
HT29
G1 G2/M
DNA content
D
Percentage of total cells
100%
50%
0%
Noco
Noco + TSA
Taxol
Taxol + TSA
DNA content
G2/M
S
G1
Sub-G1

Figure 5 (Previous page).Brief TSA treatment impairs the mitotic checkpoint invoked by spindle-disrupting drugs. Hela cells were grown on coverslips, synchronized, and three hours after release mock-treated or treated with 200 nM TSA. Either nocodazole (A) or paclitaxel (B) were then added seven hours after release. All cells were then fixed at 12 hours after release and stained for BubR1 (top panels, "BUBR1"), the centromere with human anti-centromeric sera (panels second from the top, "ACA"), and chromatin with DAPI (panels third from the top, "DAPI"). Control cells show BubR1 localization at the paired kinetochores in mitotic cells, in comparison to diminished BubR1 localization TSA-treated cells. The kinetochore localization of BubR1 coincides with the centromere, as indicated by the yellow areas when the respective pseudo-colored staining for BubR1, ACA, and DAPI are merged (bottom panels, "Merged"). Images shown of control and TSA-treated cells were captured with equal length of exposure time and are representative of at least 100 cells in each treatment group. (C) Parallel plates of Hela (top quartet of panels) or HT29 (bottom quartet of panels) cells were synchronized and released, and mock-treated (left panels) or treated with TSA (right panels) 3 hours after release, followed by either nocodazole or paclitaxel ("Taxol"). All cells were then harvested at 20 hours after release and assessed for cell cycle distribution by FACS analysis. (D) Bar graphs showing the cell-cycle distribution of cells in each treatment group in the histograms shown in (C).

contributes to abrogation of the mitotic spindle checkpoint. This in turn sensitizes otherwise checkpoint-competent cancer cells to rapid killing by microtubule-disrupting drugs. Finally, the rapid killing by the combination of TSA and microtubule-disrupting drugs ultimately results in decreased clonogenic survival. It may also be worth noting that these effects were achieved with relatively brief exposure (i.e., < 10 hours) to drugs. As the HDAC inhibitors have typically been administered in the clinic as bolus infusions, the exposure of tumor to drug is likely also time-limited, perhaps increasing the clinical relevance of our findings.

These results are in accord with previous reports that histone deacetylase inhibition perturbs aspects of mitotic progression, but do not exclude the possibility that HDI's perturb other pathways as well to bring about cell death. Cimini et al.[24] found evidence from cytological and fluorescent in situ hybridization (FISH) studies that TSA led to impaired sister chromatid separation in normal human fibroblasts,[24] and which likely contributes to chromosomal missegregation in the face of an inactivated mitotic checkpoint. Warrener et al.[25] found increased death in cells treated with the azelaic bishydroxamic acid (ABHA, an HDI unrelated to TSA), and especially when administered concurrently with nocodazole, an indication that other HDI's may abrogate the mitotic spindle checkpoint to increase cancer cell killing as well.[25] Interestingly, in the same report it was noted that a lower dose of ABHA (10 μg/mL vs 100 μg/mL) was ineffective in bypassing nocodazole-induced arrest, but prolonged mitotic transit time, an observation that we have also found true for TSA (data not shown). It is possible that the dose-threshold for mitotic checkpoint abrogation is due to the higher concentration of HDI's required to inhibit specific HDACs, such as HDAC4 or 5.[18] Other reports have found prolonged mitotic arrest and chromosomal instability, but this may be due to differences in dose or duration of HDI treatment.[47,48] Finally, it is worth emphasizing that these results are pertinent for proliferating cells in which the mitotic spindle checkpoint can be invoked. It is likely that HDIs have effects on nonproliferating cancer cells as well,[49] possibly through mechanisms such as upregulation of proapoptotic pathways and/or receptors for death-inducing ligands.[50]

What is the mechanism by which TSA mediates abrogation of the mitotic spindle checkpoint? It is likely not solely related to alteration

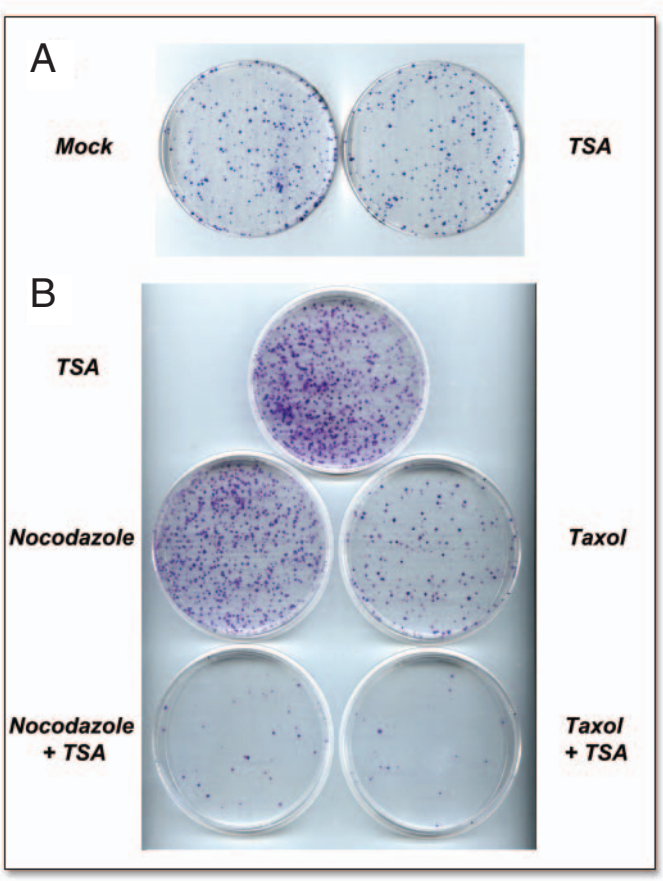

Figure 6. Brief TSA treatment leads to reduced clonogenic survival after exposure to mitotic spindle-disrupting drugs. (A) Representative plates showing colonies after mock treatment or treatment with TSA. Synchronized Hela cells were mock-treated or treated with TSA three hours after release. Seventeen hours later, all cells were washed, counted and replated into new plates with fresh drug-free media to grow undisturbed for an additional 10 days. All plates were then fixed, stained, and the colonies counted. All assays were performed in triplicate and the results averaged. (B) Representative plates showing colonies after brief treatment with TSA followed by mitotic spindle-disrupting drugs. Synchronized cells were prepared as in (A), followed by the addition of nocodazole or paclitaxel at seven hours and which was left on until 20 hours after release, at which time the cells of each treatment group were counted, replated into new plates with fresh drug-free media. Plates were left to grow undisturbed, and then fixed, stained, and assessed for colonies. All assays were performed in triplicate and the results averaged. (C) Histograms showing colony survival after the various treatments described in (A and B). Colony counts are expressed as a percentage normalized to the control untreated cells, with error bars indicating standard deviation.

of chromatin structure by TSA. TSA results in decondensation of chromatin and opening of centromeric DNA at concentrations less than 20 ng/ml,[51] while we found abrogation of the spindle checkpoint was diminished below 200 ng/ml (results not shown). A more compelling hypothesis may be that TSA leads to displacement of mitotic checkpoint proteins from the kinetochore, either due to histone hyperacetylation, the alteration of centromeric DNA, or inactivation of kinases active in mitosis such as the aurora B kinase. Lack of BubR1 localization to kinetochores, such as that resulting from RNA interference, spontaneously arising in certain cell lines, or through targeted deletion has been associated with mitotic spindle checkpoint inactivation and increased cell death.[5,6,52,53] It is intriguing

to note that the effects of TSA described here are reminiscent of hesperadin or ZM447439, small molecule inhibitors of the aurora B kinase which phosphorylates histone H3.[34,35,54-56] Treatment of cells with either agent led to reduced phosphorylation of histone H3 and BubR1 in mitotic cells, which in turn was associated with reduced BubR1 localization to kinetochores as well as chromosome missegregation and mitotic catastrophe that was accentuated with spindle-disrupting agents. Finally, while all HDACs have the ability in vitro to deacetylate core histones, in vivo substrates likely also include nonhistone proteins, the deacetylation of which may be impaired by TSA.[57,58,59]

In summary, these results we report here may have therapeutic implications in the optimal use of HDAC inhibitors, especially were they to be combine with microtubule-targeting chemotherapy. Our findings may begin to provide a mechanistic understanding of how HDIs enhances the efficacy of specific treatments, such the enhancement by HDIs of paclitaxel-induced cell death in ovarian cancer cell lines.[32] The efficacy and safety of combined treatment with microtubule-disrupting chemotherapy and HDAC inhibition will ultimately require confirmation in animal studies and in clinical trials.

References

1. Chan G, Yen TJ. The mitotic checkpoint: a signaling pathway that allows a single unattached kinetochore to inhibit mitotic exit. Prog Cell Cycle Res 2003; 5:431-9.
2. Cleveland DW, Mao Y, Sullivan KF. Centromeres and kinetochores: from epigenetics to mitotic checkpoint signaling. Cell 2003; 24:407-21.
3. Jallepalli PV, Lengauer C. Chromosome segregation and cancer: cutting through the mystery. Nat Rev Cancer 2001; 1:109-17.
4. Chan GK, Jablonski SA, Sudakin V, Hittle JC, Yen TJ. Human BUBR1 is a mitotic checkpoint kinase that monitors CENP-E functions at kinetochores and binds the cyclosome/APC. J Cell Biol 1999; 5:941-54.
5. Kops GJ, Foltz DR, Cleveland DW. Lethality to human cancer cells through massive chromosome loss by inhibition of the mitotic checkpoint. Proc Natl Acad Sci USA 2004; 1018699-704.
6. Lee EA, Keutmann MK, Dowling ML, Harris E, Chan G, Kao GD. Inactivation of the mitotic checkpoint as a determinant of the efficacy of microtubule-targeted drugs in killing human cancer cells. Mol Cancer Ther 2004; 3:661-9.
7. Sudakin V, Chan GK, Yen TJ. Checkpoint inhibition of the APC/C in HeLa cells is mediated by a complex of BUBR1, BUB3, CDC20, and MAD2. J Cell Biol 2001; 154:925-36.
8. Taylor SS, Hussein D, Wang Y, Elderkin S, Morrow CJ. Kinetochore localisation and phosphorylation of the mitotic checkpoint components Bub1 and BubR1 are differentially regulated by spindle events in human cells. J Cell Sci 2001; 114:4385-95.
9. Shannon KB, Canman JC, Salmon ED. Mad2 and BubR1 function in a single checkpoint pathway that responds to a loss of tension. Mol Biol Cell 2002; 13: 3706-19.
10. Chen RH. BubR1 is essential for kinetochore localization of other spindle checkpoint proteins and its phosphorylation requires Mad1. J Cell Biol 2002; 158:487-96.
11. Fang G. Checkpoint protein BubR1 acts synergistically with Mad2 to inhibit anaphase-promoting complex. Mol Biol Cell 2002; 13:755-66.
12. Mao Y, Abrieu A, Cleveland DW. Activating and silencing the mitotic checkpoint through CENP-E-dependent activation/inactivation of BubR1. Cell 2003; 114:87-98.
13. Babu JR, Jeganathan KB, Baker DJ, Wu X, Kang-Decker N, Van Deursen JM. Rae1 is an essential mitotic checkpoint regulator that cooperates with Bub3 to prevent chromosome missegregation. J Cell Biol 2003; 160:341-53.
14. Holloway SL, Glotzer M, King RW, Murray AW. Anaphase is initiated by proteolysis rather than by the inactivation of maturation-promoting factor. Cell 1993; 7:1393-402.
15. Kruhlak MJ, Hendzel MJ, Fischle W, Bertos NR, Hameed S, Yang XJ, Verdin E, Bazett-Jones DP. Regulation of global acetylation in mitosis through loss of histone acetyltransferases and deacetylases from chromatin. J Biol Chem 2001; 276:38307-19.
16. Krebs JE, Fry CJ, Samuels ML, Peterson CL. Global role for chromatin remodeling enzymes in mitotic gene expression. Cell 2000; 102:587-998.
17. Toth KF, Knoch TA, Wachsmuth M, Frank-Stohr M, Stohr M, Bacher CP, Muller G, Rippe K. Trichostatin A-induced histone acetylation causes decondensation of interphase chromatin. J Cell Sci 2004; 117:4277-87.
18. Furumai R, Komatsu Y, Nishino N, Khochbin S, Yoshida M, Horinouchi S. Potent histone deacetylase inhibitors built from trichostatin A and cyclic tetrapeptide antibiotics including trapoxin. Proc Natl Acad Sci USA 2001; 98:87-92.
19. Magnaghi-Jaulin L, Groisman R, Naguibneva I, Robin P, Lorain S, Le Villain JP, Troalen F, Trouche D, Harel-Bellan A. Retinoblastoma protein represses transcription by recruiting a histone deacetylase. Nature 1998; 391:601-5.
20. Gui CY, Ngo L, Xu WS, Richon VM, Marks PA. Histone deacetylase (HDAC) inhibitor activation of p21WAF1 involves changes in promoter-associated proteins, including HDAC1. Proc Natl Acad Sci USA 2004; 101:1241-6.
21. Qiu L, Burgess A, Fairlie DP, Leonard H, Parson PO, Gabrielli BO. Histone deacetylase inhibitors trigger a G2 checkpoint in normal cells that is defective in tumor cells. Mol Biol Cell 2004; 11:2069-83.
22. Kim YB, Ki SW, Yoshida M, Horinouchi S. Mechanism of cell cycle arrest caused by histone deacetylase inhibitors in human carcinoma cells. J Antibiot (Tokyo) 2000; 53:1191-200.
23. Blagosklonny MV, Robey R, Sackett DL, Du L, Traganos F, Darzynkiewicz Z, Fojo T, Bates SE. Histone deacetylase inhibitors all induce p21 but differentially cause tubulin acetylation, mitotic arrest, and cytotoxicity. Mol Cancer Ther 2002; 1:937-41.
24. Cimini D, Mattiuzzo M, Torosantucci L, Degrassi F. Histone hyperacetylation in mitosis prevents sister chromatid separation and produces chromosome segregation defects. Mol Biol Cell 2003; 14:3821-33.
25. Warrener R, Beamish H, Burgess A, Waterhouse NJ, Giles N, Fairlie D, Gabrielli B. Tumor cell-selective cytotoxicity by targeting cell cycle checkpoints. FASEB J. 2003; 17:1550-1552.
26. Piekarz RL, Robey R, Sandor V, Bakke S, Wilson WH, Dahmoush L, Kingma DM, Turner ML, Altemus R, Bates SE. Inhibitor of histone deacetylation, depsipeptide (FR901228), in the treatment of peripheral and cutaneous T-cell lymphoma: a case report. Blood 2001; 98:2865-8.
27. Yoshida M, Furumai R, Nishiyama M, Komatsu Y, Nishino N, Honouchi S. Histone deacetylase as a new target for cancer chemotherapy. Cancer Chemother Pharmacol 2001; 48:S20-6.
28. Richon VM, O'Brien JP. Histone deacetylase inhibitors: a new class of potential therapeutic agents for cancer treatment. Clin Cancer Res 2002; 8:662-4.
29. Vigushin DM, Coombes RC. Histone deacetylase inhibitors in cancer treatment. Anticancer Drugs 2002; 13:1-13.
30. Sandor V, Bakke S, Robey RW, Kang MH, Blagosklonny MV, Bender J, Brooks R, Piekarz RL, Tucker E, Figg WD, Chan KK, Goldspiel B, Fojo AT, Balcerzak SP, Bates SE. Phase I trial of the histone deacetylase inhibitor, depsipeptide (FR901228, NSC 630176), in patients with refractory neoplasms. Clin Cancer Res 2002; 8:718-28.
31. Kelly WK, Richon VM, O'Connor O, Curley T, MacGregor-Curtelli B, Tong W, Klang M, Schwartz L, Richardson S, Rosa E, Drobnjak M, Cordon-Cordo C, Chiao JH, Rifkind R, Marks PA, Scher H. Phase I clinical trial of histone deacetylase inhibitor: suberoylanilide hydroxamic acid administered intravenously. Clin Cancer Res 2003; 9: 3578-88.
32. Chobanian NH, Greenberg VL, Gass JM, Desimone CP, Van Nagell JR, Zimmer SG. Histone deacetylase inhibitors enhance paclitaxel-induced cell death in ovarian cancer cell lines independent of p53 status. Anticancer Res 2004: 539-45.
33. Marks PA, Richon VM, Kelly WK, Chiao JH, Miller T. Histone deacetylase inhibitors: development as cancer therapy. Novartis Found Symp 2004; 259:269-81.
34. Ditchfield C, Johnson VL, Tighe A, Ellston R, Haworth C, Johnson T, Mortlock A, Keen N, Taylor SS. Aurora B couples chromosome alignment with anaphase by targeting BubR1, Mad2, and Cenp-E to kinetochores. J Cell Biol 2003; 161:267-80.
35. Hauf S, Cole RW, LaTerra S, Zimmer C, Schnapp G, Walter R, Heckel A, van Meel J, Rieder CL, Peters JM. The small molecule Hesperadin reveals a role for Aurora B in correcting kinetochore-microtubule attachment and in maintaining the spindle assembly checkpoint. J Cell Biol 2003; 161:281-94.
36. Lens SM, Medema RH. The survivin/aurora B complex: its role in coordinating tension and attachment. Cell Cycle 2003; 2: 507-10.
37. Kao GD, McKenna WG, Guenther MG, Muschel RJ, Lazar MA, Yen TJ. Histone deacetylase 4 interacts with 53BP1 to mediate the DNA damage response. J Cell Biol. 2003; 160:1017-1027.
38. Kao GD, McKenna WG, Maity A, Blank K, Muschel RJ. Cyclin B1 availability is a rate-limiting component of the radiation-induced G2 delay in HeLa cells. Cancer Res 1997; 57:753-8.
39. Kao GD, McKenna WG, Muschel RJ. Mitosis-promoting factor activity is excluded from the nucleus during the Radiation-Induced G2 arrest in Hela cells. J Biol Chem 1999; 274:34779-84.
40. Roth SY, Allis CD. Histone acetylation and chromatin assembly: a single escort, multiple dances? Cell 1996; 87:5-8.
41. Martinez-Balbas MA, Dey A, Rabindran SK, Ozato K, Wu C. Displacement of sequence-specific transcription factors from mitotic chromatin. Cell 1995; 83:29-38.
42. Hans F, Dimitrov S. Histone H3 phosphorylation and cell division. Oncogene 2001; 20:3021-7.
43. Zeitlin SG, Barber CM, Allis CD, Sullivan KF, Sullivan K. Differential regulation of CENP-A and histone H3 phosphorylation in G2/M. J Cell Sci 2001; 114:653-61
44. Prigent C, Dimitrov S. Phosphorylation of serine 10 in histone H3, what for? J Cell Sci 2003; 116:3677-85.
45. Goto H, Tomono Y, Ajiro K, Kosako H, Fujita M, Sakurai M, Okawa K, Iwamatsu A, Okigaki T, Takahashi T, Inagaki M. Identification of a novel phosphorylation site on histone H3 coupled with mitotic chromosome condensation. J Biol Chem 1999:25543-9.
46. Goto H, Yasui Y, Nigg EA, Inagaki M. Aurora-B phosphorylates Histone H3 at serine28 with regard to the mitotic chromosome condensation. Genes Cells 2002; 7:11-7.
47. Taddei A, Maison C, Roche D, Almouzni O. Reversible disruption of pericentric heterochromatin and centromere function by inhibiting deacetylases. Nat Cell Biol 2001; 3:114-9.
48. Shin HJ, Baek KH, Jeon AH, Kim SJ, Jang KL, Sung YC, Kim CM, Lee CW. Inhibition of histone deacetylase activity increases chromosomal instability by the aberrant regulation of mitotic checkpoint activation. Oncogene 2003; 22:3853-8.
49. Burgess A, Ruefli A, Beamish H, Warrener R, Saunders N, Johnstone R, Gabrielli B. Histone deacetylase inhibitors specifically kill nonproliferating tumour cells. Oncogene 2004; 23:6693-701.

50. Nakata S, Yoshida T, Horinaka M, Shiraishi T, Wakada M, Sakai T. Histone deacetylase inhibitors upregulate death receptor 5/TRAIL-R2 and sensitize apoptosis induced by TRAIL/APO2-L in human malignant tumor cells. Oncogene 2004; 23:6261-71.
51. Sumer H, Saffery R, Wong N, Craig JM, Choo KH. Effects of scaffold/matrix alteration on centromeric function and gene expression. J Biol Chem 2004; 279:37631-9.
52. Dai W, Wang Q, Liu T, Swamy M, Fang Y, Xie S, Mahmood R, Yang YM, Xu M, Rao CV. Slippage of mitotic arrest and enhanced tumor development in mice with BubR1 haploinsufficiency. Cancer Res 2004; 64:440-5.
53. Baker DJ, Jeganathan KB, Cameron JD, Thompson M, Juneja S, Kopecka A, Kumar R, Jenkins RB, de Groen PC, Roche P, van Deursen JM. BubR1 insufficiency causes early onset of aging-associated phenotypes and infertility in mice. Nat Genet 2004; 36:744-9.
54. Shindo M, Nakano H, Kuroyanagi H, Shirasawa T, Mihara M, Gilbert DJ, Jenkins NA, Copeland NG, Yagita H, Okumura K. cDNA cloning, expression, subcellular localization, and chromosomal assignment of mammalian aurora homologues, aurora-related kinase (ARK) 1 and 2. Biochem Biophys Res Commun 1998; 244:285-92.
55. Adams RR, Eckley DM, Vagnarelli P, Wheatley SP, Gerloff DL, Mackay AM, Svingen PA, Kaufmann SH, Earnshaw WC. Human INCENP colocalizes with the Aurora-B/AIRK2 kinase on chromosomes and is overexpressed in tumour cells. Chromosoma 2000; 110:65-74.
56. Ota T, Suto S, Katayama H, Han ZB, Suzuki F, Maeda M, Tanino M, Terada Y, Tatsuka M. Increased mitotic phosphorylation of histone H3 attributable to AIM-1/Aurora-B overexpression contributes to chromosome number instability. Cancer Res 2002; 62:5168-77.
57. Hubbert C, Guardiola A, Shao R, Kawaguchi Y, Ito A, Nixon A, Yoshida M, Wang XF, Yao TP. HDAC6 is a microtubule-associated deacetylase. Nature 2002; 417:455-8.